Synthesis of a Novel Two-Dimensional Antimony Sulfide, $[C_4H_{10}N]_2[Sb_8S_{13}]\cdot 0.15H_2O$, and Its Structure Solution Using Synchrotron/Imaging Plate Data

Younghee Ko,[†] Kemin Tan,[†] John B. Parise,*[,†,‡] and Alex Darovsky[§]

CHiPR, Department of Earth and Space Sciences, State University of New York, Stony Brook, New York 11794; Department of Chemistry, State University of New York, Stony Brook, New York 11794; and SUNY X3 Beamline, National Synchrotron Light Source, Brookhaven National Laboratory, Upton, New York 11973

Received August 23, 1995. Revised Manuscript Received November 6, 1995[⊗]

A novel antimony sulfide, $[C_4H_{10}N]_2[Sb_8S_{13}]\cdot 0.15H_2O$, was synthesized hydrothermally, and its structure was determined from data collected using a synchrotron/imaging plate system. The new compound consists of centrosymmetric $Sb_{16}S_{26}^{4-}$ planar clusters. Each cluster is connected to four others through two edge-sharing and two corner-sharing SbS_3 pyramids, forming an extended sheet. The protonated pyrrolidine molecules reside between the parallel stacked sheets. The structure is triclinic (space group $P\bar{1}$) with $a = 6.929(2)$ Å, $b = 16.747(2)$ Å, $c = 17.976(4)$ Å, $\alpha = 94.84(1°)$, $\beta = 95.41(1)°$, and $\gamma = 125.28(1)°$.

Introduction

Recently series of main-group sulfide compounds, for example, thioantimonates,[1−16] thiostannates,[17−21] and thiogermanates[22−25] have been synthesized using hydrothermal techniques. Specifically, the thioantimonates show a remarkable variation of stoichiometries and structures. The latter can be attributed to the stereochemical effect of the inert lone pair and the tendency of Sb to adopt three, four, or five coordination. These extended frameworks promise to yield new materials with useful electrical, optical, catalytic, and ion-exchange properties.[21,22,26] In this series of new thioantimonate compounds, yellow, orange, red, and dark red materials are produced, suggesting a variety of band gaps in the range 2−3 eV;[15,27] the band gap for Sb_2S_3 is 1.7 eV.[28]

The hydrothermal syntheses of thioantimonates gives rise to a variety of chain,[9−11,15,16] layer,[2−8] and three-dimensional[1,12,14] structures; the dimensionality being determined by the presence of Sb−S bonds along 1-, 2-, or 3-noncollinear directions. Distances shorter than the sum of the corresponding van der Waals radii are used to define bonds. Most of thioantimonates are produced in the presence of alkali or alkaline earth metals,[1,2,4−10,29−31] while there a few examples of materials crystallizing from slurries containing organic molecules such as aliphatic or aromatic amines.[12,14−16,32] Systematic exploratory synthesis employing organic templates in other main-group sulfides have led to a number of novel crystalline compounds, which show structural relationships between the frameworks and the templating molecules.[18−21] The geometry of the template within the crystalline structure formed from hydrothermal treatment provides valuable information about possible templating mechanisms.

Thioantimonate phases crystallizing from slurries containing organic templates typically occur as needles or as small crystals, unsuitable for conventional single-crystal X-ray diffractometry.[15] Recent innovations in

[†] CHiPR, Center for High Pressure Research, an NSF Science and Technology Center and Department of ESS, SUNY.
[‡] Department of Chemistry, SUNY.
[§] Brookhaven National Laboratory.
[⊗] Abstract published in *Advance ACS Abstracts,* December 15, 1995.

(1) Graf, H. A.; Schäfer, H. *Z. Naturforsch.* **1972**, *27b*, 735.
(2) Dittmar, G.; Schäfer, H. *Z. Anorg. Allg. Chem.* **1978**, *441*, 93.
(3) Sheldrick, W. S., Kaub, J. *Z. Anorg. Allg. Chem.* **1986**, *536*, 114.
(4) Volk, K.; Schäfer, H. *Z. Naturforsch.* **1979**, *34b*, 172.
(5) Volk, K.; Schäfer, H. *Z. Naturforsch.* **1978**, *33b*, 827.
(6) Volk, K.; Schäfer, H. *Z. Naturforsch.* **1979**, *34b*, 1637.
(7) Sheldrick, W. S., Hausler, H.-J. *Z. Anorg. Allg. Chem.* **1988**, *561*, 149.
(8) Sheldrick, W. S., Hauser, H.-J. *Z. Anorg. Allg. Chem.* **1988**, *557*, 105.
(9) Dittmar, G.; Schäfer, H. *Z. Anorg. Allg. Chem.* **1978**, *441*, 98.
(10) Graf, H. A.; Schäfer, H. *Z. Anorg. Allg. Chem.* **1975**, *414*, 211.
(11) Volk, K.; Bickert, P.; Kolmer, R.; Schäfer, H. *Z. Naturforsch.* **1979**, *34b*, 380.
(12) Wang, X.; Liebau, F. *J. Solid State Chem.* **1994**, 385.
(13) Parise, J. B. *J. Chem. Soc., Chem. Commun.* **1990**, 1553.
(14) Parise, J. B. *Science* **1991**, *251*, 292.
(15) Parise, J. B.; Ko, Y. *Chem. Mater.* **1992**, *4*, 1446.
(16) Tan, K.; Ko, Y.; Parise, J. B. *Acta Crystallogr.* **1994**, *C50*, 1439.
(17) Sheldrick, W. S.; Braunbeck, H. G. *Z. Naturforsch.* **1989**, *4b*, 851.
(18) Jiang, T.; Lough, A. J.; Ozin, G. A.; Young, D. *Chem. Mater.* **1995**, *7*, 245.
(19) Ko, Y.; Cahill, Christopher, L.; Parise, J. B. *J. Chem. Soc., Chem. Commun.* **1994**, 69.
(20) Ko, Y.; Tan, K.; Nellis, D. M.; Koch, S.; Parise, J. B. *J. Solid State Chem.* **1994**, *114*, 506.
(21) Parise, J. B.; Ko, Y.; Rijssenbeck, J.; Nellis, D. M.; Tan, K.; Koch, S. *J. Chem. Soc., Chem. Commun.* **1994**, 527.
(22) Bedard, R. L.; Wilson, S. T.; Vail, L. D.; Bennett, J. M.; Flanigen, E. M. In *Zeolites: Facts, Figures, Future. Proceedings of the 8th International Zeolite Conference*; Elsevier: Amsterdam, 1989; p 375.
(23) Nellis, D. M.; Ko, Y.; Tan, K.; Koch, S.; Parise, J. B. *J. Chem. Soc., Chem. Commun.* **1995**, 541.
(24) Tan, K.; Darovsky, A.; Parise, J. B. *J. Am. Chem. Soc.* **1995**, *117*, 7039.
(25) Yaghi, O. M.; Richardson, A.; Groy, T. L. *J. Am. Chem. Soc.* **1994**, *116*, 807.
(26) Ozin, G. A.; A. Kuperman; Stein, A. *Angew. Chem., Int. Ed. Engl.* **1989**, *28*, 359.
(27) McCarthy, T. J.; Kanatzidis, M. G. *Inorg. Chem.* **1994**, *33*, 1205.
(28) Bube, R. H. *Photoconductivity of solids*; John Wiley and Sons, Inc.: New York: 1960; p 233.
(29) Eisenmann, B.; Schäfer, H. *Z. Naturforsch.* **1979**, *34b*, 383.
(30) Cordier, G.; Schwidetzky, C.; Schafer, H. *J. Solid State Chem.* **1984**, *54*, 84.
(31) Sheldrick, W. S.; Hauser, H. J. *Z. Anorg. Allg. Chem.* **1988**, *557*, 98.
(32) Wang, X. *Eur. J. Solid State Inorg. Chem.* **1995**, *32*, 303.

0897-4756/96/2808-0493$12.00/0

Table 1. Selected Crystallographic Data for the Synchrotron/Imaging Plate Experiment for Pyr-SbS-SB7

Crystal Data	
chem formula	$[C_4H_{10}N]_2[Sb_8S_{13}]\cdot 0.15H_2O$
chem formula weight	1537.8
cryst system	triclinic
space group	$P\bar{1}$
unit cell	$a = 6.929(2)$ Å, $b = 16.747(2)$ Å, $c = 17.976(4)$ Å, $\alpha = 94.84(1)°$, $\beta = 95.41(1)°$, $\gamma = 125.28(1)°$
vol of unit cell	1670.3(8) Å^3
formula per unit cell, Z	2
density calcd from formula and cell	3.057 g mm^{-3}
radiation type and wavelength	synchrotron, $\lambda = 0.642(1)$ Å
no. of reflns for cell meast and 2θ range	26 reflns, $11.6° < 2\theta < 39.6°$
meast temp	293 K
crystal shape, color, and size	triclinic, dark red 0.02 × 0.02 × 0.06 mm
Data Collection	
data collection method	imaging plate
imagining plate	Fuji imaging plate, medical, high resolution, HR-V, 20 × 25 cm
scanner	Fuji, bioimaging analyzer, BAS2000
gradation	1024
latitude	4
resolution	100 μm
sensitivity	10 000
oscillation angle	7°
overlap angle	1°
ϕ range	360°
no. of images	60
no. of reflns integrated ($I > 1.0\sigma(I)$)	11 777
no. of independent reflns	6042
merge R (based on I)	0.029
min, max value of θ	5.56°, 29.84°
abs correction	none
Refinement	
refinement on	F
final R, R_w	0.045, 0.040
S	2.00
no. of parameters refined	284
no. of reflections used	5004 ($\theta_{max} = 25.5°$)
weighting scheme	$w = [\sigma^2(I) + 0.0009I^2]^{-1/2}$
max (Δ/σ)	0.01
max residual electron density	2.06 e Å^{-3}

synchrontron imaging plate (IP) technology[33−35] have allowed the structural characterization of crystals in the size range 10−30 μm.[24] In this report, we describe the structure of $[C_4H_{10}N]_2[Sb_8S_{13}]\cdot 0.15H_2O$, labeled type 7 by Parise and Ko in the publication describing its synthesis.[15] The phase was designated Pyr-SbS-SB7 following the nomenclature established for the sulfide frameworks by workers at Union Carbide.[22] The structure of this material has been resolved using IP data collected using the NSLS synchrotron source.

Experimental Section

Synthesis and Characterization. Pyrrolidine (Aldrich-Chemical) was used in an attempt to direct the recrystallization of Sb_2S_3 (Aldrich Chemical). Sb_2S_3 (0.454 g) was first mixed with H_2O (0.53 g). The pyrrolidine (0.069 g) was reacted completely with elemental sulfur (0.031 g). The mixtures were then combined and heated at 160 °C under thiosulfate bearing hydrothermal conditions in a Pyrex-lined bomb for 3 days. Dark red crystals were recovered, washed with a water−ethanol solution, and dried in air. The yield was 90% based on Sb_2S_3. The powder X-ray diffraction pattern indicated the presence of Pyr-SbS-SB7.[15] The positions and intensities of the calculated X-ray powder diffraction pattern from the structure described in this paper are very similar to those of the observed pattern (Figure 1).

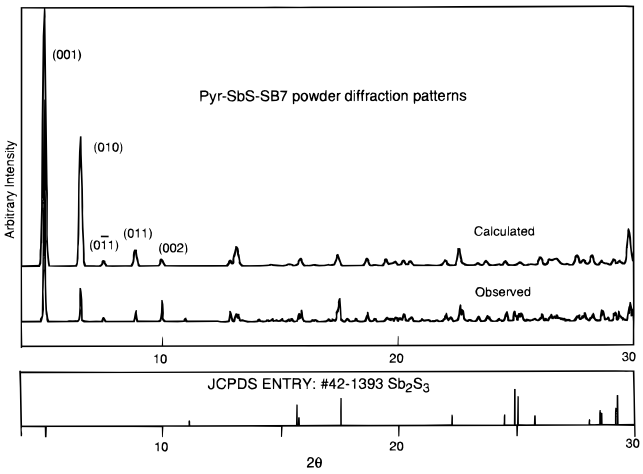

Figure 1. (a) Calculated (top) and observed (bottom) X-ray powder diffraction patterns of Pyr-SbS-SB7, Cu Kα radiation. The experiment was performed on a Scintag diffractometer. (b) The JCPDS[44] entry for the pattern of Sb_2S_3, an impurity in the powder used for this study.

Anion chromatography of the pyrrolidine/sulfur starting solution showed a predominance of $S_2O_3^{2-}$ and small amounts of SO_4^{2-} and SO_3^{2-} species. Amines and elemental sulfur, when combined in water, tend to produce thiosulfate.[36] In contrast, HCO_3^- and HS^- have been used as optimum mineralizers for thioantimonates in previous hydrothermal studies.[1−17]

(33) Handu, J.; Machin, P. A.; Campbell, J. W.; Greenhough, T. J.; Clifton, I. J.; Zurek, S.; Gover, S.; Johnson, L. N.; Elder, M. *Nature* **1987**, *329*, 178.

(34) Miyahara, J.; Takahashi, K.; Amemiya, Y.; Kamiya, N.; Satow, Y. *Nucl. Instrum. Methods* **1986**, *A246*, 572.

(35) Sakabe, N. *Nucl. Instrum. Methods* **1991**, *303*, 448.

(36) Arntson, R. H.; Dickson, F. W.; Tunell, G. *Am. J. Sci.* **1958**, *258*, 574.

Table 2. Fractional Coordinates ($\times 10^4$) and Isotropic Atomic Displacement Parameters for Pyr-SbS-SB7

atom	*x*	*y*	*z*	B_{eq}/B_{iso}[a]
Sb(1)	6660.6(10)	5137.0(4)	3110.0(3)	1.4(1)
Sb(2)	2135.1(10)	5130.9(5)	1699.3(3)	1.7(1)
Sb(3)	6894.7(10)	3066.3(5)	3721.6(4)	1.7(1)
Sb(4)	2647.5(10)	3521.7(5)	4622.5(3)	1.5(1)
Sb(5)	2405.6(10)	5887.5(5)	3804.2(3)	1.4(1)
Sb(6)	7002.8(10)	953.8(4)	4201.2(4)	1.7(1)
Sb(7)	3157.8(10)	1281.8(5)	5412.7(4)	1.8(1)
Sb(8)	3080.0(11)	5283.9(5)	−423.6(4)	2.0(1)
S(1)	2409(4)	4268(2)	3113(1)	1.6(1)
S(2)	6325(4)	3605(2)	2526(1)	1.8(1)
S(3)	6332(4)	5721(2)	1885(1)	1.7(1)
S(4)	2523(4)	6453(2)	2549(1)	1.9(1)
S(5)	2690(4)	6148(2)	679(1)	2.2(1)
S(6)	2735(4)	2124(2)	3946(1)	1.6(1)
S(7)	6083(4)	1491(2)	3040(1)	2.2(1)
S(8)	6774(4)	6824(2)	4038(1)	1.4(1)
S(9)	2841(4)	56(2)	4436(1)	1.7(1)
S(10)	6405(4)	−480(2)	3473(1)	2.1(1)
S(11)	7414(4)	2577(2)	5565(1)	1.9(1)
S(12)	2445(4)	3874(2)	85(1)	2.1(1)
S(13)	6911(4)	4688(2)	4675(1)	1.4(1)
N(1)	10463(15)	2065(6)	2150(5)	2.4(2)
N(2)	10887(18)	8084(8)	2545(6)	3.7(3)
C(1)	10108(29)	1099(11)	1942(9)	5.5(5)
C(2)	8792(139)	741(24)	1148(14)	28.6(42)
C(3)	8305(77)	1345(22)	902(13)	16.8(18)
C(4)	9579(32)	2322(11)	1467(7)	5.5(5)
C(5)	11787(27)	8211(12)	1791(8)	5.2(5)
C(6)	10723(55)	8751(21)	1411(11)	10.3(11)
C(7)	8754(36)	8535(14)	1811(10)	6.3(6)
C(8)	9483(26)	8458(13)	2608(8)	5.9(5)
O(1)	12083(181)	504(80)	1677(59)	9.3(25)

[a] B_{iso} is for O(1) only. The site occupancy of O(1) is 0.14(2). $B_{eq} = (8\pi^2/3)\sum_i\sum_j U_{ij} a_i a_j \mathbf{a}_i^* \cdot \mathbf{a}_j$.

Quantitative electron probe microanalysis (EPMA) indicated the presence of Sb and S in a molar ratio of 8:13; this result was subsequently confirmed by the analysis of single-crystal X-ray diffraction data. Thermogravimetric analysis (TGA) was carried out using a Perkin-Elmer thermal analysis system. An 8.135 mg sample was heated under nitrogen at the rate of 2.0 °C/min from room temperature to 400 °C. A weight loss of 9.75%, presumably due to pyrrolidine (calcd 9.53%) was observed, between and 260 °C. The X-ray powder diffraction of material recovered following these experiments matched that for Sb_2S_3, indicating the collapse of the sulfide framework.

X-ray Experiment. The synchrotron/imaging plate data were collected at the X3A1 beamline of the National Synchrontron Light Source (NSLS). First, a set of 26 reflections was measured with a scintillation counter to obtain a precise orientation matrix and cell parameters. To collect the data, an image plate cassette was mounted on the detector arm, replacing the scintillation counter. The experimental details were described in a previous paper[24] and experimental parameters are listed in the Table 1.

The orientation matrix was used to index reflections on the imaging plates. After each image was processed to obtain the refined crystal-to-plate distance and the IP tilt angles,[37] a total of 11 777 fully recorded reflections with $I > 1.0\sigma(I)$ were integrated using the "seed-skewness" method.[38] Those close to the oscillation axis, IP margins or oscillation boundaries were rejected. Reflections were merged[39] in point group $\bar{1}$ (R_{merge} = 2.9% based on intensity) resulting in 6042 unique data. The statistical intensity distribution of reflections strongly indicated a centrosymmetric symmetry.

Structure Determination. The structure was solved in space group $P\bar{1}$ using the direct methods routines in Shelxs-86.[40] The subsequent refinement was carried out using a package of programs written and maintained by Calabrese.[41] Besides atoms in the $Sb_8S_{13}^{2-}$ framework, two crystallographically unique pyrrolidine molecules were found in Fourier difference maps. For charge balance, these two molecules were assumed to be protonated, $C_4H_{10}N^+$, though H atoms on the organic templates were not located in this study. Additionally, a major isolated peak was assigned to an O atom from a H_2O molecule with partial site occupancy. Since Pyr-SbS-SB7 was obtained through hydrothermal reaction, some water molecules are expected to occupy the open space within the framework. Other major residual peaks with electron density ranging from 1.52 to 2.06 e Å^{-3} were found 0.829−1.018 Å away from Sb atoms. The results of the final refinements are summarized in the Table 1. The atomic coordinates and geometric parameters are listed in Tables 2 and 3.

Table 3. Selected Geometric Parameters (Å, deg) for Pyr-SbS-SB7

Sb(1)−S(1)	2.418(2)	S(1)···N(1)[e]	3.342(9)
Sb(1)−S(2)	2.559(3)	S(2)···N(1)[e]	3.270(9)
Sb(1)−S(3)	2.527(2)	S(3)···N(2)	3.332(10)
Sb(2)−S(3)	2.447(2)	S(7)···N(1)	3.240(9)
Sb(2)−S(4)	2.444(3)	S(10)···N(2)[f]	3.268(10)
Sb(2)−S(5)	2.513(3)		
Sb(3)−S(2)	2.483(3)	S(1)−Sb(1)−S(2)	95.25(8)
Sb(3)−S(6)	2.456(2)	S(1)−Sb(1)−S(3)	91.66(8)
Sb(3)−S(7)	2.527(3)	S(2)−Sb(1)−S(3)	97.20(8)
Sb(4)−S(6)	2.580(2)	S(3)−Sb(2)−S(4)	99.73(8)
Sb(4)−S(8)[a]	2.572(2)	S(3)−Sb(2)−S(5)	92.75(8)
Sb(4)−S(13)	2.408(2)	S(4)−Sb(2)−S(5)	85.99(9)
Sb(5)−S(4)	2.510(2)	S(2)−Sb(3)−S(6)	98.46(8)
Sb(5)−S(8)	2.442(2)	S(2)−Sb(3)−S(7)	93.44(9)
Sb(5)−S(11)[a]	2.650(3)	S(6)−Sb(3)−S(7)	90.01(8)
Sb(6)−S(7)	2.511(3)	S(6)−Sb(4)−S(8)[a]	94.66(8)
Sb(6)−S(9)	2.466(2)	S(6)−Sb(4)−S(13)	90.22(8)
Sb(6)−S(10)	2.423(3)	S(8)a−Sb(4)−S(13)	92.32(7)
Sb(7)−S(9)	2.479(2)	S(4)−Sb(5)−S(8)	90.37(8)
Sb(7)−S(10)[b]	2.592(3)	S(4)−Sb(5)−S(11)[a]	89.01(8)
Sb(7)−S(11)	2.416(2)	S(8)−Sb(5)−S(11)[a]	92.59(8)
Sb(8)−S(5)	2.482(3)	S(7)−Sb(6)−S(9)	92.68(8)
Sb(8)−S(12)[c]	2.534(3)	S(7)−Sb(6)−S(10)	93.0(1)
Sb(8)−S(12)	2.418(3)	S(9)−Sb(6)−S(10)	95.06(8)
		S(9)−Sb(7)−S(10)[b]	93.57(8)
Sb(1)···S(8)	3.113(2)	S(9)−Sb(7)−S(11)	99.10(8)
Sb(1)···S(13)	2.987(2)	S(10)b−Sb(7)−S(11)	94.25(9)
Sb(2)···S(1)	3.071(3)	S(5)−Sb(8)−S(12)	100.53(9)
Sb(2)···S(12)	3.536(3)	S(5)−Sb(8)−S(12)[c]	97.64(9)
Sb(3)···S(11)	3.515(3)	S(12)−Sb(8)−S(12)[c]	87.95(8)
Sb(3)···S(13)	3.080(2)	Sb(1)−S(1)−Sb(5)	99.69(8)
Sb(4)···S(1)	3.110(3)	Sb(1)−S(2)−Sb(3)	98.16(8)
Sb(4)···S(13)[a]	2.985(2)	Sb(1)−S(3)−Sb(2)	100.96(8)
Sb(5)···S(1)	2.888(2)	Sb(2)−S(4)−Sb(5)	101.6(1)
Sb(5)···S(13)[a]	3.058(2)	Sb(2)−S(5)−Sb(8)	104.0(1)
Sb(6)···S(9)[b]	3.120(3)	Sb(3)−S(6)−Sb(4)	101.18(8)
Sb(6)···S(11)	3.366(3)	Sb(3)−S(7)−Sb(6)	96.2(1)
Sb(7)···S(6)	3.160(3)	Sb(4)a−S(8)−Sb(5)	98.83(7)
Sb(7)···S(8)[a]	3.215(3)	Sb(6)−S(9)−Sb(7)	101.81(8)
Sb(8)···S(3)[c]	3.185(2)	Sb(6)−S(10)−Sb(7)[b]	98.7(1)
Sb(8)···S(5)[d]	3.215(3)	Sb(5)a−S(11)−Sb(7)	100.21(8)
		Sb(8)−S(12)−Sb(8)[c]	92.05(8)
		Sb(4)−S(13)−Sb(1)	96.76(7)

[a] $1-x, 1-y, 1-z$. [b] $1-x, -y, 1-z$. [c] $1-x, -y, -z$. [d] $-x, 1-y, 1-z$. [e] $-1+x, y, z$. [f] $-1+x, -1+y, -z$.

Results and Discussion

The structure contains eight unique Sb(III) atoms. Each is coordinated to three S atoms with bond lengths ranging from 2.408(2) to 2.650(3) Å, forming a trigonal-pyramidal primary building unit. As shown in Figure 2, these corner shared pyramids form a centrosymmetric

(37) Bolotovsky, R., personal communication.
(38) Bolotovsky, R.; White, M. A.; Darovsky, A.; Coppen, P. *J. Appl. Cryst.* **1995**, *28*, 86.
(39) Blessing, R. H. *J. Appl. Cryst.*, **1989**, *22*, 396 and references therein.
(40) Sheldrick, G. M. *Acta Crystallogr.* **1990**, *A46*, 467−473.
(41) Calabrese, J. C. The Z package of programs, EI DuPont, Wilmington, DE.

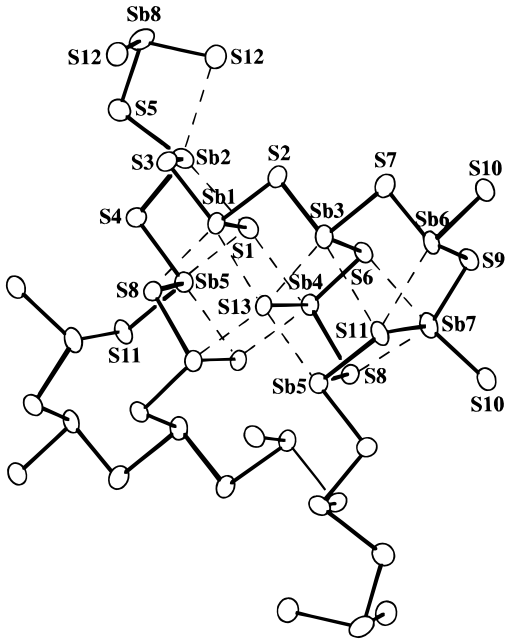

Figure 2. Centrosymmetric $Sb_{16}S_{26}^{4-}$ planar cluster in the $[C_4H_{10}N]_2[Sb_8S_{13}]\cdot 0.15H_2O$ (Pyr-SbS-SB7) structure. The short Sb−S bonds (from 2.408 to 2.650 Å) are drawn in dark lines, while the longer Sb−S bonds (from 2.888 to 3.536 Å) are drawn in dash lines to show the fused semicubes and cubes. The displacement ellipsoids in this ORTEP[45] drawing are scaled to enclose 50% probability.

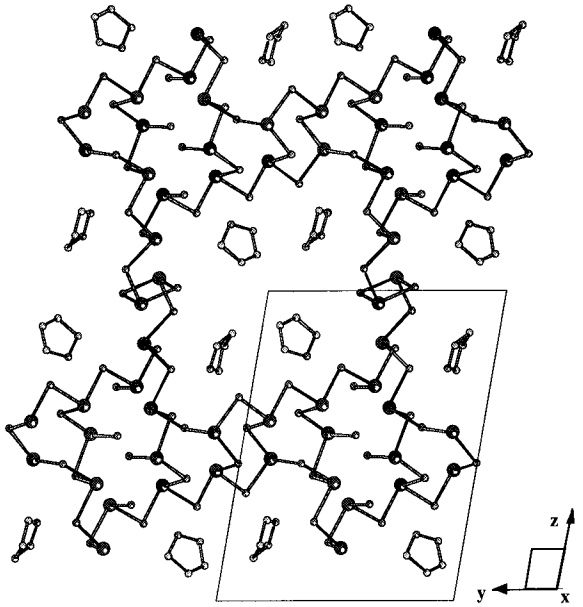

Figure 3. Sheet structure of $[C_4H_{10}N]_2[Sb_8S_{13}]\cdot 0.15H_2O$ (Pyr-SbS-SB7). Each $Sb_{16}S_{26}^{4-}$ cluster is connected to four others through two edge-sharing and two corner-sharing SbS_3 pyramids. The connections between clusters are also made by fused semicubes. Two crystallographic unique pyrrolidine molecules, which are assumed to be protonated, are within the parallelogram-shaped apertures and between the sheets, which are stacked parallel to [100].

$Sb_{16}S_{26}^{4-}$ cluster. All antimony atoms have two additional long Sb−S bonds with bond lengths from 2.888(2) to 3.515(2) Å (Figure 2). These distances are considerably shorter than the sum of the Sb−S van der Waals radii (4.05 Å).[41] This type of (3 + 2) coordination, the three short Sb−S bonds with two additional sulfur atoms at distances from 2.888(2) to 3.515(2) Å, is observed in Sb_2S_3,[42] $Sb_3S_5\cdot N(C_3H_7)_4$,[15] and $Sb_8S_{13}\cdot[CH_3NH_3]_2$.[12]

The $Sb_{16}S_{26}^{4-}$ cluster (Figure 2) consists of four fused cubes (for example, one forms from Sb3, S6, Sb4, S13, Sb5, S8, Sb7, and S11) six fused semicubes (for example, the site labeled Sb2, S3, Sb1, S1, S8, Sb5, and S4) and two individual pyramids. This cluster is connected to four others by fused cubes or semicubes (Figure 2) forming a planar $Sb_{16}S_{26}^{4-}$ unit and the extended $Sb_8S_{13}^{2-}$ sheet shown in Figure 3. The semicube building unit occurs in other hydrothermally synthesized antimony and tin sulfides.[14,18−21] Secondary building units consisting of both fused cubes and semicubes are also found in $[CH_3NH_3]_2Sb_8S_{13}$.[12] However, unlike $[CH_3NH_3]_2Sb_8S_{13}$,[12] the compound incorporating $[C_4H_{10}N]^+$ does not form a three-dimensional network. Instead, the structure (Figure 3) consists of layers in (100) containing apertures about 11.0 Å × 11.5 Å. The thickness of the layer is about 2.5 Å with protonated pyrrolidine molecules residing in the space between them. The shortest distance between two atoms from two neighboring sheets is 3.215 Å. The distances between nitrogen in the pyrrolidine and sulfur attached to the framework range from 3.240(9) to 3.342(9) Å, indicating the hydrogen bonding between the template molecule and the framework.[16,23]

Conclusion

A new framework with the composition $[Sb_8S_{13}]^{2-}$ has been synthesized hydrothermally in the presence of pyrrolidine. The structure of this compound has been solved from a small single crystal (20 × 20 × 60 μm) using synchrotron/imaging plate data. Recent innovations in synchrotron/imaging plate technology have allowed the investigation of crystals previously considered too weakly diffracting for crystallographic studies.

Acknowledgment. We thank the National Science Foundation (DMR 94-13003) for support. Research carried out in part at the National Synchrotron Light Source at Brookhaven National Laboratory which is supported by the U.S. Department of Energy, Division of Materials Sciences and Division of Chemical Sciences. The SUNY X3 beamline at the NSLS is supported by the Division of Basic Energy Sciences of the U.S. Department of Energy (DE-FG02-86ER45231).

Supporting Information Available: Tables of crystallographic data (3 pages); list of observed and calculated structure factor amplitudes (7 pages). Ordering information is given on any current masthead page.

CM950402J

(42) Pauling, L. *The nature of the chemical bond*; Cornell University Press: Ithaca, NY, 1966; p 260.
(43) Hofmann, W. *Z. Kristallogr.* **1933**, *86*, 225.
(44) JCPDS *Powder Diffraction File—Inorganic Phases*; International Centre for Diffraction Data: 1601 Park Lane, Swartmore, PA 19081-2389, 1988.
(45) Johnson, C. K. ORTEP reported ORNL-3764; Oak Ridge National Laboratory, Oak Ridge, TN, 1965.